Journal of Quantitative Spectroscopy & Radiative Transfer 124 (2013) 11–20

Contents lists available at SciVerse ScienceDirect

Journal of Quantitative Spectroscopy & Radiative Transfer

journal homepage: www.elsevier.com/locate/jqsrt

Line strengths and updated molecular constants for the C_2 Swan system

James S.A. Brooke [a,*], Peter F. Bernath [a,b], Timothy W. Schmidt [c], George B. Bacskay [c]

[a] Department of Chemistry, University of York, Heslington, York, YO10 5DD, UK
[b] Department of Chemistry & Biochemistry, Old Dominion University, 4541 Hampton Boulevard, Norfolk, VA 23529-0126, USA
[c] School of Chemistry, Building F11, The University of Sydney, New South Wales 2006, Australia

ARTICLE INFO

Article history:
Received 7 December 2012
Received in revised form
20 February 2013
Accepted 21 February 2013
Available online 6 March 2013

Keywords:
Diatomic molecules
C_2
Swan system
Line strengths
Einstein *A*
Oscillator strengths
f-values
Line lists

ABSTRACT

New rotational line strengths for the C_2 Swan system ($d^3\Pi_g - a^3\Pi_u$) have been calculated for vibrational bands with $v' = 0-10$ and $v'' = 0-9$, and J values up to $J = 34-96$, using previous observations in 33 vibrational bands. Line positions from several sources were combined with the results from recent deperturbation studies of the $v' = 4$ and $v' = 6$ levels, and a weighted global least squares fit was performed. The updated molecular constants are reported. The line strengths are based on a recent ab initio calculation of the transition dipole moment function. A line list has been made available, including observed and calculated line positions, Einstein *A* coefficients and oscillator strengths (*f*-values). The line list will be useful for astronomers, combustion scientists and materials scientists who utilize C_2 Swan spectra. Einstein *A* coefficients and *f*-values were also calculated for the vibrational bands of the Swan system.

1. Introduction

C_2 is an important molecule in the fields of astronomy, combustion science and materials science. It has often been observed in comets [1–6] and in other astronomical environments such as interstellar clouds [7–13], late-type stars [14–17] and the Sun [18,19]. Its reactions are believed to be involved in the formation of hydrocarbons and other organic compounds in interstellar clouds [20]. C_2 has also been found in flames [21–23] and from the irradiation of soot [24], and can be formed in carbon plasmas and used to make carbon nanostructures [25].

The most prominent electronic system in the visible region is the Swan system, which involves the electronic transition $d^3\Pi_g - a^3\Pi_u$, with the (0,0) band near 19 400 cm^{-1}. The $a^3\Pi_u$ state was originally believed to be the ground state [26] as it was observed to be easily excited, which is because it lies only about 700 cm^{-1} above the actual $X^1\Sigma_g^+$ ground state (this difference being that between the T_v values of $v = 0$ for each state).

The Swan system has been investigated extensively. Early vibrational band intensity analyses include those of King [27], Phillips [28] and Hagan [29]. In 1965, Mentall and Nicholls [30] reanalysed the data of three previous works to provide an updated list of absolute band strengths, oscillator strengths and Einstein *A* values for most vibrational bands up to $v' = 4$. A full review of previous work was given in 1967 by Tyte et al. [31]. In 1968, Phillips and Davis [32] combined earlier published data with their most recent rotational analysis. They calculated spectroscopic constants for the Swan system, and published a full rotational line list including relative intensities. Danylewych and Nicholls published a list of absolute band strengths, oscillator strengths and Einstein

* Corresponding author. Tel.: +44 1904 434525.
E-mail address: jsabrooke@gmail.com (J.S.A. Brooke).

0022-4073/$ - see front matter © 2013 Elsevier Ltd. All rights reserved.
http://dx.doi.org/10.1016/j.jqsrt.2013.02.025

Table 1
Perturbation constants[a] for the $d^3\Pi_g$, $v'=4$ and $v'=6$ levels of the C_2 Swan system. Those of Bornhauser et al. [45,46], and those resulting from the fit of all molecular constants are reported.

Parameter	Bornhauser et al. value	Value from fit[b]
$\langle d^3\Pi_g, v'=4 \vert H_{SO} \vert b^3\Sigma_g^-, v'=16\rangle$	−0.6401(86)	−0.6147(59)
$\langle d^3\Pi_g, v'=4 \vert BL_+ \vert b^3\Sigma_g^-, v'=16\rangle$	0.24737(61)	0.24869(21)
$\langle d^3\Pi_g, v'=6 \vert H_{SO} \vert b^3\Sigma_g^-, v'=19\rangle$	0.7855(110)	0.7417(82)
$\langle d^3\Pi_g, v'=6 \vert BL_+ \vert b^3\Sigma_g^-, v'=19\rangle$	0.31192(37)	0.31123(12)
$\langle d^3\Pi_g, v'=6 \vert H_{SO} \vert 1^5\Pi_g\rangle$	4.6220(88)	4.6150(94)

[a] Numbers in parentheses indicate one standard deviation to the last significant digits of the constants.
[b] Note that these values were floated to improve the fit, but the studies of Bornhauser et al. were directly aimed at calculating these constants.

A values covering most vibrational bands of up to $v'=9$, with $\Delta v \le 4$ [33]. The properties of C_2 were extensively reviewed by Huber and Herzberg in 1979 [34].

As new experimental techniques have become available, new studies of the lower vibrational bands have been conducted at high resolution. These include the work of Amiot [35], Curtis and Sarre [36] and Suzuki et al. [37], who investigated the (0–0), (0–1) and (1–0) bands, respectively, using laser excitation techniques. Dhumwad et al. [38] observed the Swan system using a quartz discharge tube with tungsten electrodes for the excitation of CO. In 1994, Prasad and Bernath [39] analysed nine low vibrational bands ($v' \le 3$ and $v'' \le 4$) of the Swan system of jet-cooled C_2 (for low-J), and of C_2 produced in a composite wall hollow cathode (for *J* up to 25–46) with a Fourier Transform Spectrometer (FTS). The previous observations of Amiot et al. and Prasad and Bernath on the (0,0) band were improved upon by Lloyd and Ewart in 1999 [40], using degenerate four-wave mixing spectroscopy. These and other investigations have improved the accuracy of the line assignments originally published by Phillips and Davis in 1968 [32].

The higher vibrational bands had not been analyzed with modern high resolution instrumentation until 2002, when Tanabashi and Amano [41] observed the Swan system by a direct absorption technique using a tunable dye laser. They measured three bands, assigned as (5,7), (6,8) and (7,9). They found that their line positions did not agree with those reported by Phillips and Davis [32], which was the most recent rotational analysis of the high vibrational bands. These discrepancies led to the reanalysis of the entire Swan system with a high resolution FTS [42]. The assigned line positions from this new comprehensive analysis agreed with their previous one for the (5,7), (6,8) and (7,9) bands. Moreover, their line positions for other bands involving the higher vibrational levels differed significantly from those of Phillips and Davis [32].

The old rotational line list reported by Phillips and Davis in 1968 [32] has recently been used in deriving the carbon abundance and $^{12}C/^{13}C$ ratio in R Coronae Borealis and hydrogen-deficient carbon stars [17], and in comets [43]. Line positions and intensities must be known to derive abundances from observed spectra, and it would be beneficial to have a new rotational line list, based on recent measurements and calculations. The purpose of this work is to use the data mainly of Tanabashi et al. [42] to calculate theoretical line intensities, and publish an extensive line list. Similar work has recently been carried out for the $E^2\Pi$-$X^2\Sigma^+$ transitions of CaH by Li et al. [44]

Tanabashi et al. assigned around 5700 observed rotational lines, for 34 vibrational bands belonging to the $\Delta v=-3$ to $+2$ sequences. Transitions up to between $J=30$ and 80 were assigned. Perturbations were found in the $d^3\Pi_g$ state for $v=0$, 1, 2, 4, 6, 8, 9 and 10, and for $v=4$, 6 and 9 they affected almost all of the observed lines. They calculated molecular constants (Tables 3 and 4 in Ref. [42]) for both electronic states.

Deperturbation studies of the $d^3\Pi_g$ $v'=4$ [45] and $v'=6$ [46] levels were performed by Bornhauser et al. in 2010 and 2011, respectively, using double-resonant four-wave mixing spectroscopy. This enabled them to assign lines unambiguously, and calculate perturbation constants (Table 1) and molecular constants (Table 2) of the interacting $b^3\Sigma_g^-$ ($v=16$ and $v=19$) and $1^5\Pi_g$ states. They also gave a list of the few transitions that were assigned incorrectly by Tanabashi et al. Recently, the (4,8) and (5,9) bands were observed by Yeung et al. [47] using high resolution laser absorption spectroscopy.

In this current paper, the molecular constants from Tanabashi et al. are improved slightly using the data from the deperturbation studies, but the main focus is the calculation of line intensities using these constants and theoretical methods. This enables the production of a comprehensive line list that can be used by those in the fields of astronomy, combustion science and materials science to calculate abundances from C_2 Swan spectra.

Table 2
Molecular constants[a] for the $b^3\Sigma_g^-$, $v'=16$ and $v'=19$ and $1^5\Pi_g$ states, which perturb the $d^3\Pi_g$, $v'=4$ and $v'=6$ levels. Those of Bornhauser et al. [45,46], and those resulting from the fit of all molecular constants are reported.

State	Parameter	Bornhauser et al. value	Value from fit
$b^3\Sigma_g^-$, $v=16$	*T*	26191.865(14)	26191.1742(29)
	B	1.22858(15)	1.233492(68)
	$D\times10^6$	6.4351(fixed)[b]	6.4351(fixed)[b]
	λ	0.172(18)	0.335(17)
$b^3\Sigma_g^-$, $v=19$	*T*	29442.1348(843)	29442.589(14)
	B	1.179368(214)	1.178182(49)
	$D\times10^6$	6.5066(fixed)[b]	6.5066(fixed)[b]
	λ	0.142(22)	0.135(26)
$1^5\Pi_g$	*T*	29258.5922(48)	29258.5824(65)
	B	1.14413(11)	1.14442(11)
	A	8.9450(47)	8.9428(54)
	λ	−0.0428(23)	−0.0427(27)
	o	−0.0744(39)	−0.0812(44)

[a] Numbers in parentheses indicate one standard deviation to the last significant digits of the constants.
[b] As with Bornhauser et al., these *D* constants were fixed at values extrapolated from the molecular constants of Amiot et al. [51].

2. Recalculation of molecular constants

With the recent publication of perturbation constants for the $d^3\Pi_g$ $v=4$ and $v=6$ levels by Bornhauser et al. [45,46] (Table 1), there was an opportunity to improve the molecular constants reported by Tanabashi et al. (Tables 3 and 4 in Ref. [42]). The computer program *PGOPHER* [48], written by C. M. Western (University of Bristol) was used to recalculate the molecular constants, with the inclusion of the $v'=4$ and $v'=6$ perturbations, using the standard N^2 Hamiltonian for a $^3\Pi$ state [49,50]. A global least squares fit was performed including all lines from Tanabashi et al., Tanabashi and Amano [41], Prasad and Bernath [39], Curtis and Sarre [36], Suzuki et al. [37], Lloyd and Ewart [40] (for the (0,0) band), the two deperturbation studies by Bornhauser et al. (both the Swan system lines and the transitions between the perturbing states and the $a^3\Pi_u$ state), and most lines from Yeung et al. [47] (see below).

2.1. The (4,8) and (5,9) bands

Yeung et al. observed 153 and 121 transitions in the (4,8) and (5,9) bands, respectively [47]. They reported that the (5,9) band was unperturbed and that line assignment was simple, and so all of these lines were included in our fit. The (4,8) band however was heavily perturbed. To help in assigning the lines, they attempted to use the perturbation constants from Bornhauser et al. [45,46] to estimate line positions, but could not find agreement with a number of lines. Ultimately, they assigned all of the lines without the use of the perturbation constants. They gave two examples of transitions, $R_1(9)$ and $R_2(8)$ (reported to be at 13 907.568 and 13 905.145 cm^{-1}), for which no lines could be found in the region of the calculated positions. Using molecular constants directly from Tanabashi et al., these line positions are calculated as 13 907.821 and 13 905.788 cm^{-1}, respectively, and with the inclusion of the Bornhauser et al. perturbation constants, this changes to 13 904.778 and 13 907.437 cm^{-1}, respectively. Therefore, there is a line in their data in the region of the estimated (perturbation included) position for the $R_2(8)$ transition (at 13 907.568 cm^{-1}). For the $R_1(9)$ transition, the closest reported line is 0.37 cm^{-1} away at 13 905.145 cm^{-1}. Also, the reported positions are still 0.25 and 0.64 cm^{-1} away from the expected positions using Tanabashi et al. [42] molecular constants only. In fact, the average difference between the expected positions using Tanabashi et al. molecular constants only and those reported by Yeung et al., for all (4,8) lines that were retained in our fit, was as high as 0.44 cm^{-1}.

The inclusion of the perturbation constants improves the residuals of all of the lines of the Swan system that Bornhauser et al. observed. Therefore, many of the (4,8) lines seem to have been incorrectly assigned by Yeung et al. However, the line positions have an accuracy of 0.003 cm^{-1}, and so it was considered worthwhile to investigate the assignments and include as many of the lines as possible in our fit.

To check their assignments, a preliminary fit was performed using all other data described (including the perturbation constants) to estimate positions for the (4,8) band. This showed 19 (of 153) transitions whose assigned positions were more than 0.5 cm^{-1} away from the estimated value. The observed positions were compared with all nearby calculated values with the aim of changing assignments, if there was only one obvious option. 7 positions were reassigned, and most of the other positions either had several nearby options and so could not confidently be reassigned, or had already been assigned to a more likely transition as well (and noted as an overlapped line). Only 3 lines had no nearby (within 0.1 cm^{-1}) options. Due to the lack of confidence in the assignments, any lines that differed significantly from their calculated values and could not be reassigned were removed from the fit. The fit was continued, and any lines whose residuals were greater than 0.03 cm^{-1} were then removed. This process was repeated iteratively until no lines differed by more than 0.03 cm^{-1}. The entire process was repeated several times, using the updated constants as the starting point. 100 of the initial 153 lines remained after this treatment. This removed a number of correctly assigned lines, but also decreased the chance of including any incorrect ones in the fit.

2.2. Data included in the global fit

In their calculation of molecular constants in 2007 [42], Tanabashi et al. included lines from several other studies. For nine bands up to (3,4), gaps in observations were filled in by using lines from Prasad and Bernath [39]. High resolution measurements of the (0,1) band by Curtis and Sarre [36] were included, as were cross transitions ($\Delta\Omega\neq 0$) from Suzuki et al. [37] for the (1,0) band. Some cross transitions were also observed by Curtis and Sarre, and these are particularly useful for the accurate calculation of the spin-orbit coupling and Λ-doubling constants. All lines from Tanabashi and Amano [41] for the (5,7), (6,8) and (7,9) bands were also included.

Prasad and Bernath also calculated molecular constants, and included in their fit all lines from Curtis and Sarre, Suzuki et al. and Amiot (for the (0,0) band). Our recalculation is based mainly on that of Tanabashi et al., and also this fit by Prasad and Bernath. An explanation of the specific differences is presented below.

The weights for the lines from Tanabashi et al. (including those from Tanabashi and Amano) were unchanged here, except for those involving the $v'=4$ and $v'=6$ levels. These had mostly been deweighted, and were weighted more strongly in this study as the perturbations had been included in the fit. In their calculation of the perturbation constants, Bornhauser et al. [45,46] observed lines involving $J'=1-6$, 10–12 and 17–23 for the $v'=6$ level, and $J'=4-14$ for the $v'=6$ level. Lines involving these J levels were weighted highly, and other line weights were decreased with greater difference between their J' level and these ranges. The actual lines observed by Bornhauser et al. were weighted similarly to those of Tanabashi et al. for the same bands. The lines for both bands observed by Yeung et al. [47] were weighted based on the reported accuracy (0.003 cm^{-1}). Lines marked as overlapped by Yeung et al. were slightly deweighted.

Table 3
Updated molecular constants[a] for the $d^3\Pi_g$ state of the C_2 Swan system (in cm^{-1}).

v	T	A	A_D	B	$D\times10^6$	λ	o	p	q
0	19 378.46749(51)	−14.00139(63)	0.0005068(83)	1.7455663(43)	6.8205(16)	0.03301(47)	0.61076(52)	0.003973(43)	−0.0007752(43)
1[b]	21 132.14977(25)	−13.87513(49)	0.0005740(83)	1.7254062(53)	7.0194(77)	0.02972(38)	0.61713(36)	0.004133(44)	−0.0008171(43)
2	22 848.3877(21)	−13.8205(23)	0.000600(43)	1.704516(21)	7.308(22)	0.0253(41)	0.6208(32)	0.00624(38)	−0.000835(14)
3	24 524.2201(19)	−13.5361(28)	0.000775(17)	1.681437(16)	7.438(24)	0.0470(26)	0.5827(26)	0.00579(17)	−0.0008568(85)
4	26 155.0448(29)	−13.3892(50)	0.001451(14)	1.656859(26)	7.684(43)	0.0219(38)	0.6313(32)	0.00954(29)	−0.000923(21)
5	27 735.6720(43)	−13.0324(66)	0.000723(37)	1.630205(23)	8.573(32)	0.0601(28)	0.6161(23)	0.00685(32)	−0.000912(15)
6	29 259.3548(36)	−12.820(10)	0.001203(56)	1.599876(31)	8.998(44)	0.0529(71)	0.5773(71)	0.00874(47)	−0.000986(22)
7	30 717.9011(46)	−12.3458(71)	0.000814(41)	1.566047(32)	10.044(66)	0.0960(34)	0.5532(31)	0.00936(35)	−0.001175(17)
8	32 102.655(22)	−12.107(22)	0.00076(fixed)	1.52675(31)	9.60(97)	0.095(fixed)	0.546(22)	0.0055(21)	−0.00088(21)
9	33 406.230(22)	−11.698(39)	0.00076(fixed)	1.485755(96)	11.85(10)	0.172(26)	0.498(28)	0.0097(14)	−0.002062(44)
10	34 626.7860(94)	−11.297(15)	0.00076(fixed)	1.441138(72)	12.837(73)	0.115(16)	0.399(12)	0.00745(90)	−0.000977(30)

[a] Numbers in parentheses indicate one standard deviation to the last significant digits of the constants.
[b] In addition, $H=2.14(30)\times10^{-11}$ for $v=1$ was used to obtain a good fit.

Table 4
Updated molecular constants[a] for the $a^3\Pi_u$ state of the C_2 Swan system (in cm^{-1}).

v	T	A	A_D	B	$D\times10^6$	λ	o	p	q
0[b]	0	−15.26986(43)	0.0002634(71)	1.6240452(44)	6.4506(19)	−0.15450(36)	0.67525(35)	0.002537(42)	−0.0005281(44)
1	1618.02244(53)	−15.25197(61)	0.0002266(73)	1.6074266(44)	6.4439(21)	−0.15373(51)	0.67017(51)	0.002705(44)	−0.0005772(42)
2	3212.72793(96)	−15.2328(15)	0.0001996(94)	1.5907513(61)	6.4527(44)	−0.1526(12)	0.6649(14)	0.003132(77)	−0.0006457(48)
3	4784.0688(31)	−15.1972(39)	0.000186(42)	1.574088(24)	6.455(24)	−0.1333(61)	0.6815(51)	0.00488(42)	−0.000618(17)
4	6332.1364(51)	−15.2043(65)	0.000318(36)	1.557117(31)	6.338(39)	−0.1551(72)	0.6674(67)	0.00632(36)	−0.000894(16)
5	7856.8175(32)	−15.2096(35)	0.00025(fixed)	1.540139(24)	6.312(35)	−0.1492(36)	0.6546(37)	0.00734(25)	−0.001246(12)
6	9358.1565(40)	−15.1646(60)	0.000355(33)	1.523439(26)	6.034(38)	−0.1551(46)	0.6886(38)	0.00504(32)	−0.000676(16)
7	10 836.1430(92)	−15.085(11)	0.00025(fixed)	1.50869(25)	3.51(92)	−0.1641(90)	0.704(14)	−0.0244(23)	0.00632(49)
8	12 290.7997(29)	−15.1702(46)	0.00025(fixed)	1.488684(28)	5.329(52)	−0.1665(36)	0.6742(30)	0.01449(29)	−0.002053(23)
9	13 722.0897(43)	−15.0980(61)	0.000419(31)	1.472818(24)	6.066(35)	−0.1584(27)	0.6926(23)	0.00303(33)	−0.000081(16)

[a] Numbers in parentheses indicate one standard deviation to the last significant digits of the constants.
[b] In addition, $H=6.73(16)\times10^{-12}$, $o_D=-6.86(114)\times10^{-6}$ and $q_D=-9.60(41)\times10^{-9}$ were used for $v=0$ to obtain a good fit.

The five remaining sets of lines were treated as follows. The sets from Prasad and Bernath (two sets), Curtis and Sarre and Suzuki et al. were given the same weights as in the fit performed by Prasad and Bernath. Lloyd and Ewart [40] lines were assigned weights to be similar to those of Tanabashi et al. for the (0,0) band. To ensure that all lines were on the same wavenumber scale, transitions from these five sets were then compared to matching Tanabashi et al. transitions, and a weighted average wavenumber difference (one for each set) using matching lines was calculated, based on the assigned weights. This was added to all of the lines from each set as a wavenumber offset, to compensate for any systematic differences between studies. In their fit, Tanabashi et al. deweighted many lines due to the extensive perturbations, and those lines were also deweighted here if they were present in these five sets. This process excluded approximately 11% of these lines. To further decrease the possibility of using any misassigned lines in the fit, any line whose wavenumber differed from a matching Tanabashi et al. line by more than 0.03 cm^{-1} was deweighted, excluding a further $\sim$6%. A preliminary fit was then performed to obtain calculated values of each transition. Lines that had not been matched to Tanabashi et al. transitions were then deweighted if their observed minus calculated values, as a result of this fit, were greater than 0.03 cm^{-1}.

A final global weighted least squares fit was performed, in which all reported molecular constants for the $a^3\Pi_u$ and $d^3\Pi_g$ were floated, except for A_D for $v'=8$, 9 and 10, A_D for $v''=5$, 7 and 8, and λ for $v'=8$. These were fixed at values based on those calculated for the other levels to obtain a good fit. The updated molecular constants are shown in Tables 3 and 4. The magnitudes of the perturbation constants reported by Bornhauser et al. and the constants for the perturbing states were also floated to improve the fit, and both the previous and changed values are shown in Table 2. Bornhauser et al. fixed the D constants for the $b^3\Sigma_g^-$ state at values extrapolated from the molecular constants of Amiot et al. [51], and the same was done here.

3. Calculation of line intensities

The intensities of the rovibronic transitions are reported here as both Einstein A values and oscillator strengths (f-values).

Einstein A values are calculated [52] with the following equation:

$$A_{J'\rightarrow J''}=\frac{16\pi v^3 S_{J''}^{\Delta J}}{3\epsilon_0 hc^3(2J'+1)}\langle\psi_{v'J'}|R_e(r)|\psi_{v''J''}\rangle^2 \quad (1)$$

$$= 3.136\ 189\ 32 \times 10^{-7} \frac{\tilde{\nu}^3 S_{J''}^{\Delta J}}{(2J'+1)} |\langle \psi_{\nu' J'} | R_e(r) | \psi_{\nu'' J''} \rangle|^2, \quad (2)$$

where $S_{J''}^{\Delta J}$ is the Hönl–London factor and $|\langle \psi_{\nu' J'} | R_e(r) | \psi_{\nu'' J''} \rangle|$ is the transition dipole moment (TDM) matrix element, $A_{J' \to J''}$ is in s^{-1}, $\tilde{\nu}$ in cm^{-1} and R_e in Debye. These have been converted into *f*-values using the equation

$$f_{J' \leftarrow J''} = \frac{m_e \epsilon_0 c (2J'+1)}{2\pi e^2 (100\tilde{\nu})^2 (2J''+1)} A_{J' \to J''} \quad (3)$$

$$f_{J' \leftarrow J''} = 1.499\ 193\ 68\ \frac{1}{\tilde{\nu}^2} \frac{(2J'+1)}{(2J''+1)} A_{J' \to J''}. \quad (4)$$

Band intensities are reported as Einstein $A_{v'v''}$ values, and can be converted from these to $f_{v'v''}$ values using the equation:

$$f_{v' \leftarrow v''} = 1.499\ 193\ 68\ \frac{1}{\tilde{\nu}^2} A_{v' \to v''} \quad (5)$$

where $\tilde{\nu}$ is the average wavenumber for the band [53].

PGOPHER [48] was used to calculate Einstein *A* values. It is able to calculate the necessary rotational TDMs and Hönl–London factors (Eq. (1)) for several types of electronic transitions, including $^3\Pi - ^3\Pi$, if provided with a set of molecular constants and band strengths for each vibrational band.

For a diatomic molecule, the wavefunctions ψ_{vJ} used in the calculation of the TDM can be described as a one-dimensional function of internuclear distance [52]. Rotationless TDMs were calculated using the computer program *LEVEL* [54], written by Le Roy, which is able to calculate eigenfunctions and eigenvalues by solving the one-dimensional Schrödinger equation for diatomic molecules. *LEVEL* is able to calculate Einstein A values for rotational levels above $J=0$, but it assumes a singlet-singlet transition. For this reason, a single TDM (for $Q(0)$) for each vibrational band was taken from *LEVEL* and input into *PGOPHER*.

LEVEL must be provided with a potential energy curve, $V(r)$, and an electronic TDM, both as a function of internuclear distance.

3.1. Electronic transition dipole moment

Our calculation of the electronic TDM of the Swan system has been reported previously [55–57], with the results shown in Table 6 and Fig. 2. A brief description is given here. Wavefunctions were computed using the multi-reference configuration interaction (MRCI) method [58,59], whereby all single and double excitations from a complete active space self-consistent field (CASSCF) [60,61] reference state are included in the MRCI wave functions. The active space included all molecular orbitals (MO) arising from the C atoms' 2s and 2p valence orbitals. The basis set is the augmented correlation-consistent polarized aug-cc-pV6Z set of Dunning and co-workers [62–65] and de Jong et al. [66]. Core and core-valence (CV) correlation corrections were obtained using the aug-cc-pCVQZ basis set [62–64]. Scalar relativistic energy corrections (Rel) were evaluated via the Douglas–Kroll–Hess approach [67–69], in conjunction with the appropriate cc-pVQZ basis sets. The transition moments were computed by utilizing the technique of bi-orthogonal transformation [70] of the mutually non-orthogonal orbitals of the two states. These quantum chemical calculations were carried out using the MOLPRO2006.1 program [71].

3.2. Potential energy curves

The potentials $V(r)$ (Fig. 1) were calculated using the computer program *RKR1* [72], which utilizes the first-order semiclassical Rydberg–Klein–Rees procedure [73–76] to determine a set of classical turning points for each potential, using the equilibrium expansion constants ω_e, $\omega_e x_e$, $\omega_e y_e$, $\omega_e z_e$, α_e, γ_e and δ_e for B_v and $G(v)$. Values for these constants were calculated (Table 5) in a weighted least squares fit using the energy level expressions for a vibrating rotator:

$$G(v) = \omega_e(v+\tfrac{1}{2}) - \omega_e x_e(v+\tfrac{1}{2})^2 + \omega_e y_e(v+\tfrac{1}{2})^3 + \omega_e z_e(v+\tfrac{1}{2})^4 \quad (6)$$

and

$$B_v = B_e - \alpha_e(v+\tfrac{1}{2}) + \gamma_e(v+\tfrac{1}{2})^2 + \delta_e(v+\tfrac{1}{2})^3 \quad (7)$$

and the updated B_v and $G(v)$ values in Tables 3 and 4. The weightings of the vibrational levels were based on the standard deviation of B_v and $G(v)$ values from the *PGOPHER* line position fit.

3.3. Vibrational band intensities

Einstein $A_{v'v''}$ values for each vibrational band were also calculated, and are shown in Table 8. They were calculated as the sum of all single rotational Einstein *A*

Table 5
Equilibrium molecular constants[a] for the C_2 Swan system.

Constant	$d^3\Pi_g$	$a^3\Pi_u$
ω_e	1788.45(33)	1641.3463(55)
$\omega_e x_e$	16.87(19)	11.6595(19)
$\omega_e y_e$	−0.259(36)	−0.00079(16)
$\omega_e z_e$	−0.0396(20)	–
B_e	1.755408(92)	1.632355(78)
α_e	0.01960(13)	0.016582(63)
γ_e	−0.000144(39)	−0.0000273(75)
δ_e	−0.0000806(31)	–

[a] Numbers in parentheses indicate one standard deviation to the last significant digits of the constants.

Table 6
Calculated transition dipole moment function for the C_2 Swan system.

r (au)	R_e (au)	r (au)	R_e (au)	r (au)	R_e (au)	r (au)	R_e (au)
1.50	1.15048	2.25	0.94723	2.70	0.67689	3.30	0.08683
1.60	1.13942	2.30	0.92430	2.75	0.63482	3.40	0.00847
1.70	1.12242	2.35	0.89994	2.80	0.58959	3.50	−0.06088
1.80	1.10056	2.40	0.87406	2.85	0.54125	3.60	−0.12274
1.90	1.07442	2.45	0.84653	2.90	0.49020	3.70	−0.17787
2.00	1.04372	2.50	0.81717	2.95	0.43709	3.80	−0.22590
2.10	1.00858	2.55	0.78578	3.00	0.38287	3.90	−0.26485
2.15	0.98935	2.60	0.75212	3.10	0.27558	4.00	−0.29146
2.20	0.96887	2.65	0.71591	3.20	0.17578		

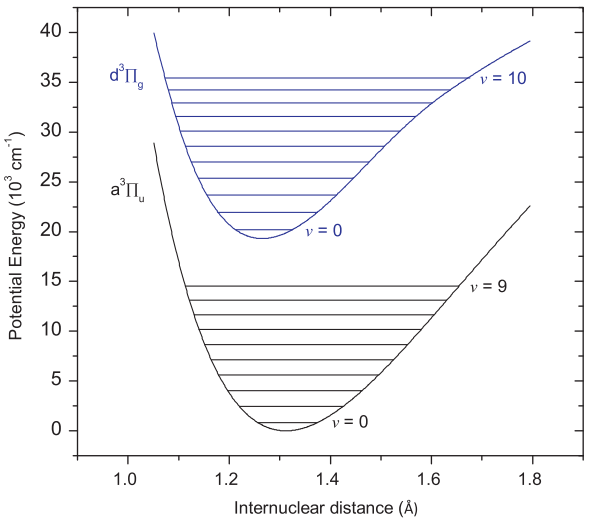

Fig. 1. The potential energy curves of the C_2 Swan system.

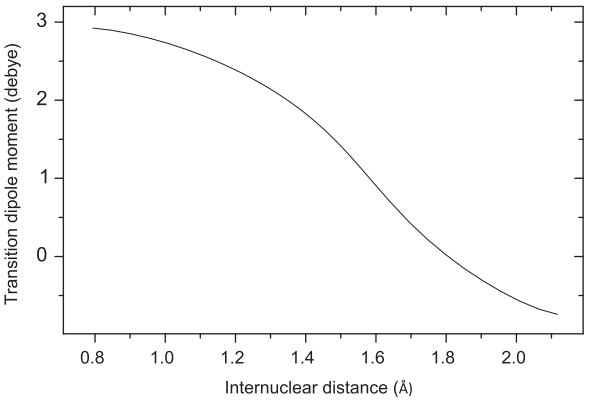

Fig. 2. The electronic transition dipole moment of the C_2 Swan system.

values for possible transitions within the relevant band from the $J'=1$, $\Omega'=0$ level. These were converted into $f_{v'v''}$ values using Eq. (5).

4. Analysis and discussion

Our final line list including positions, *f*-values and Einstein *A* values is available in the online supplementary material. The *PGOPHER* input and output files are available from the first two authors upon request. Calculated line positions and lower state energies are included for all lines, and observed positions are present when available. Line intensities are reported as both Einstein *A* values and *f*-values. Positions and intensities were calculated for all possible bands involving the observed vibrational levels (i.e. up to (0,9), (10,0) and (10,9)).

4.1. Spectral validation

PGOPHER [48] was also used for the purpose of validation, as it is able to calculate and plot spectra based on a line list. Spectra were calculated and compared to those recorded by Tanabashi et al. [42]. In all of the calculated spectra shown, a constant Gaussian instrument function was added to best match the observed broadening. The experimental procedure that Tanabashi et al. used involved observing C_2 emission from a microwave discharge in a flow of acetylene (C_2H_2) diluted in argon through a discharge tube. In such a system the molecular vibration, and to a lesser extent the rotation, will not be at thermal equilibrium. For this reason, the rotational and vibrational temperatures of the simulation were also adjusted for best agreement. Two spectra were recorded, one for the $\Delta v=-1$ to $+2$ sequences and another for the $\Delta v=-2$ and -3 sequences. Rotational and vibrational temperatures of 1140 K and 6800 K, and 940 K and 5000 K were used for the $\Delta v=-1$ to $+2$ and $\Delta v=-2$ to -3 spectra, respectively. The final parameter that had to be added manually was a linear scaling factor, as the y-axis units of the recorded spectrum are arbitrary. This value could not be kept constant during the production of each figure given below (Figs. 3–5). This is due to the presence of an instrument response function, which cannot be corrected for at this point.

The spectra match very well for the lower vibrational and rotational levels; most of the inaccuracies mentioned are present in the higher vibrational and rotational levels. Three small sections of the spectra are shown in Figs. 3–5 that are typical of the rest of the range.

Table 7
Lifetimes of vibrational levels of the C_2 $d^3\Pi_g$ state.

v'	Our value (ns)	Theoretical[a] [56] (ns)	Expt. [80] (ns)	Expt. [81] (ns)
0	98.0	95.1	101.8 ± 4.2	106 ± 15
1	99.8	96.7	96.7 ± 5.2	105 ± 15
2	102.4	99.1	104.0 ± 17	
3	106.0	102		
4	110.9	107		
5	118.2	113		

[a] The theoretical values (of Schmidt and Bacskay) include transitions to the $c^3\Sigma_u^+$ state. They state that this system contributes 3–4% to their radiative lifetimes. If this is taken into account, excellent agreement with our values is shown.

4.2. $d^3\Pi_g$ perturbations

Rotational perturbations were identified in the $d^3\Pi_g$ $v=0$–2 levels by Callomon and Gilby in 1963 [77], through their observations of the C_2 Swan system. They identified the main perturbing state as $b^3\Sigma_g^-$ (upper state of the Ballik–Ramsay system), and also suggested that a level within the $v'=0$ level could be perturbed by an as yet undiscovered $^1\Delta^g$ state (now $B^1\Delta_g$ [78]). Phillips identified further perturbations in these levels and in $v'=4-6$ in 1968 [79], and similarly identified the perturbing state as $b^3\Sigma_g^-$, though he also suggested that the $X^1\Sigma_g^+$ ground state could be perturbing $v'=0$. In 1983, Amiot investigated the (0,0) band [35] and gave further information about perturbations due to the $b^3\Sigma_g^-$ state, explained that the $X^1\Sigma_g^+$ state could not be perturbing $v'=0$, and also suggested the unidentified $^1\Delta^g$ state

Table 8
Einstein $A_{v'v''}$ values[a] of the C_2 Swan system.

	v'										
v''	0	1	2	3	4	5	6	7	8	9	10
0	7.626 (+6)	2.814 (+6)	2.809 (+5)	4.333 (+3)	2.033 (+2)	3.642 (+1)	2.470 (−2)	2.140 (−1)	9.989 (−4)	3.827 (−3)	3.140 (−9)
1	2.135 (+6)	3.427 (+6)	4.072 (+6)	6.429 (+5)	8.720 (+3)	1.608 (+3)	1.591 (+2)	4.744 (+0)	1.822 (+0)	4.947 (−2)	3.540 (−2)
2	3.832 (+5)	2.746 (+6)	1.270 (+6)	4.422 (+6)	9.615 (+5)	7.432 (+3)	6.154 (+3)	3.223 (+2)	6.379 (+1)	4.108 (+0)	1.567 (+0)
3	5.590 (+4)	8.273 (+5)	2.568 (+6)	3.236 (+5)	4.301 (+6)	1.168 (+6)	1.085 (+3)	1.805 (+4)	1.707 (+2)	3.472 (+2)	1.346 (−2)
4	7.224 (+3)	1.710 (+5)	1.169 (+6)	2.066 (+6)	2.505 (+4)	4.005 (+6)	1.149 (+6)	4.993 (+3)	3.581 (+4)	1.535 (+2)	9.452 (+2)
5	8.592 (+2)	2.886 (+4)	3.215 (+5)	1.352 (+6)	1.510 (+6)	1.513 (+4)	3.459 (+6)	1.120 (+6)	5.272 (+4)	4.975 (+4)	4.445 (+3)
6	9.574 (+1)	4.280 (+3)	6.793 (+4)	4.745 (+5)	1.381 (+6)	1.038 (+6)	8.028 (+4)	3.438 (+6)	8.558 (+5)	1.863 (+5)	4.075 (+4)
7	1.006 (+1)	5.775 (+2)	1.218 (+4)	1.218 (+5)	6.009 (+5)	1.302 (+6)	6.443 (+5)	1.343 (+5)	3.253 (+6)	4.834 (+5)	4.111 (+5)
8	9.931 (−1)	7.206 (+1)	1.945 (+3)	2.582 (+4)	1.830 (+5)	6.840 (+5)	1.087 (+6)	4.546 (+5)	1.285 (+5)	3.081 (+6)	1.342 (+5)
9	9.005 (−2)	8.335 (+0)	2.828 (+2)	4.785 (+3)	4.495 (+4)	2.421 (+5)	6.721 (+5)	9.993 (+5)	3.120 (+5)	8.080 (+4)	2.824 (+6)

[a] The numbers in parentheses indicate the exponent.

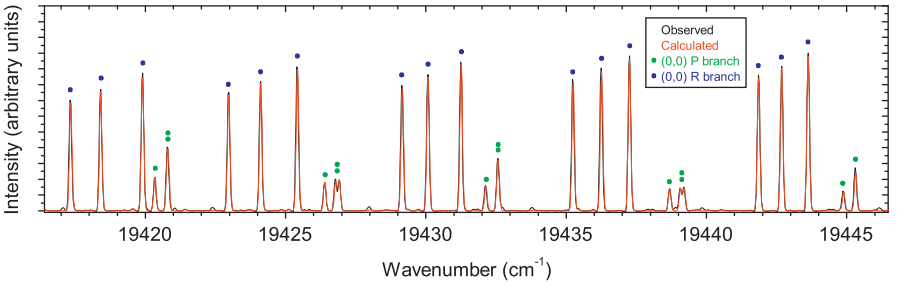

Fig. 3. A section of the (0,0) band of the C_2 Swan system. P branch: $J''=36-41$, R branch: $J''=7-13$.

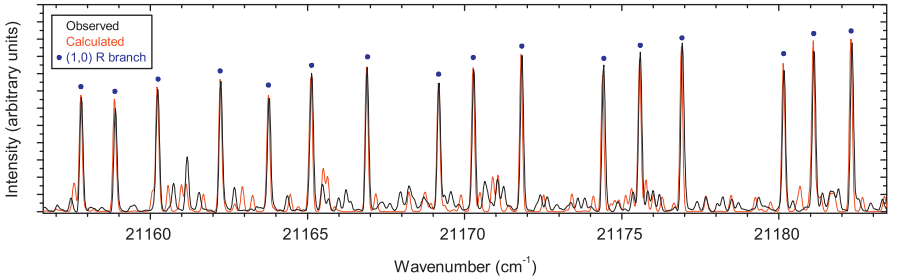

Fig. 4. A section of the $\Delta v=+1$ sequence of the C_2 Swan system, showing that the (1,0) R branch lines match well. The less intense lines do not match as closely. They are a mixture of the (1,0) P branch, the (9,8) R branch and the (8,7) P branch. (1,0) R branch: $J''=39-45$.

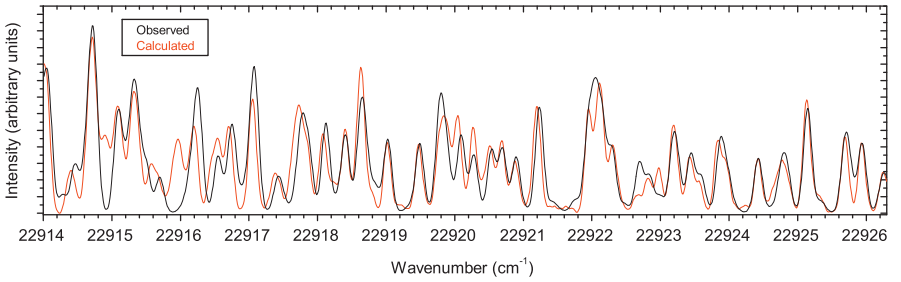

Fig. 5. A section of the $\Delta v=+2$ sequence of the C_2 Swan system. Shown is a mixture of the (2,0) R branch, the (3,1) R and P branches, the (4,2) and the P branch, (5,3) P branch, (6,4) P branch.(2,0) R branch: $J''=13-16$, (3,1) R branch: $J''=47-51$, (3,1) P branch: $J''=2-4$, (4,2) P branch: $J''=5-12$ and 39-48, (5,3) P branch: $J''=5-17$ and 45–52, (6,4) P branch: $J''=1-5$.

($B^1\Delta_g$) as a possible perturbing state. Tanabashi et al. in 2007 [42] observed numerous perturbations in $v'=0-2$, 4, 6 and 8–10, and they agreed with the above identifications by Callomon and Gilby and Amiot. They confirmed that the $B^1\Delta_g$ state was perturbing a $v'=0$ level as suggested by Callomon and Gilby and Amiot, and

also suggested that it may be perturbing some $v'=2$ levels. Most other perturbations were believed to be caused by the $b^3\Sigma_g^-$ state. The previously mentioned deperturbation studies in 2010 [45] and 2011 [46] then quantified the perturbations between the $d^3\Pi_g$ $v=4$ and $b^3\Sigma_g^-$ $v=16$ levels, and the $d^3\Pi_g$ $v=6$ and $b^3\Sigma_g^-$ $v=19$ levels. They also observed and quantified perturbations between $d^3\Pi_g$ $v=6$ and a new electronic state, $1^5\Pi_g$. Detailed descriptions of the specific perturbed rotational lines are available in the above references.

The numerous perturbations have caused many of the line positions calculated by *PGOPHER* to be slightly inaccurate, and in turn have also had a small effect on the reported intensities. With the inclusion of the perturbation constants for the $v'=4$ and $v'=6$ levels, the average error for lines involving those upper levels is improved from 0.210 to 0.069 cm^{-1}, and 0.571 to 0.038 cm^{-1}, respectively. The average error for all included lines was improved from 0.071 to 0.025 cm^{-1} The first values were calculated using the molecular constants of Tanabashi et al. and the second using those in Tables 3 and 4, excluding any lines that had been heavily deweighted in the final fit. The average error for all of the (4,8) lines that were included was reduced to 0.01 cm^{-1}. These improvements are due to the perturbation studies of Bornhauser et al. [45,46].

4.3. Updated molecular constants

As was seen by Tanabashi et al. [42], the major molecular constants *T*, *B* and *A* show a reasonably smooth vibrational dependence; the smoothness for *A* for the $d^3\Pi_g$ state has improved from Tanabashi et al., specifically with a change in $v'=6$ level. This improvement is presumably due to the inclusion of the perturbations. The other constants still show several irregularities, particularly for $v''=7-9$ and $v'=9-10$. This is unsurprising as many fewer unperturbed/deperturbed observations are available for these levels. Some A_D constants showed a large uncertainty when floated, and so were fixed at estimated values based on the other more certain A_D values. This applied to $v''=5$, 7 and 8 and $v'=8$, 9 and 10. The same was also done for the spin–spin coupling constant λ for $v'=8$.

4.4. Vibrational band Einstein A and f-values

For further validation, lifetimes of vibrational levels have been calculated and are compared to previous theoretical and experimental results in Table 7. For each upper vibrational level, lifetimes were calculated as the reciprocal of the sum of the Einstein *A* values for all possible transitions from the $J'=1$, $\Omega'=0$ level. Good agreement is shown with both sets of data. The theoretical values of Schmidt and Bacskay include transitions to the $c^3\Sigma_u^+$ state. They state that this system contributes 3–4% to their radiative lifetimes, and if this is taken into account, excellent agreement with our values is shown. Our Einstein $A_{v'v''}$ values were converted into $f_{v'v''}$ values,

Table 9
$f_{v'v''}$ values[a] of the C_2 Swan system (a), compared to those of Schmidt et al. [56] (b).

	v'											
	0		1		2		3		4		5	
v''	a	b	a	b	a	b	a	b	a	b	a	b
0	3.045 (−2)	3.069 (−2)	9.450 (−3)	9.414 (−3)	8.067 (−4)	7.885 (−4)	1.080 (−5)	9.656 (−6)	4.455 (−7)	5.104 (−7)	7.100 (−8)	6.854 (−8)
1	1.015 (−2)	1.015 (−2)	1.350 (−2)	1.374 (−2)	1.355 (−2)	1.353 (−2)	1.837 (−3)	1.786 (−3)	2.172 (−5)	1.838 (−5)	3.536 (−6)	3.794 (−6)
2	2.199 (−3)	2.185 (−3)	1.283 (−2)	1.287 (−2)	4.939 (−3)	5.146 (−3)	1.460 (−2)	1.462 (−2)	2.739 (−3)	2.650 (−3)	1.853 (−5)	1.407 (−5)
3	3.936 (−4)	3.878 (−4)	4.642 (−3)	4.618 (−3)	1.180 (−2)	1.190 (−2)	1.245 (−3)	1.379 (−3)	1.412 (−2)	1.421 (−2)	3.326 (−3)	3.201 (−3)
4	6.365 (−5)	6.204 (−5)	1.171 (−3)	1.154 (−3)	6.428 (−3)	6.403 (−3)	9.361 (−3)	9.529 (−3)	9.560 (−5)	1.417 (−4)	1.311 (−2)	1.325 (−2)
5	9.707 (−6)	9.338 (−6)	2.456 (−4)	2.392 (−4)	2.145 (−3)	2.113 (−3)	7.296 (−3)	7.288 (−3)	6.764 (−3)	6.987 (−3)	5.741 (−5)	2.853 (−5)

[a] It should be noted that in the calculation of these values, a wavenumber for the band had to be used. The value chosen was the wavenumber at which the forbidden *Q*(0) transition would appear. If the use of different wavenumbers here or $f_{v'v''}$ values for other bands are desired, the Einstein $A_{v'v''}$ values in Table 8 can be used in conjunction with Eq. (5) to calculate new $f_{v'v''}$ values. The numbers in parentheses indicate the exponent.

also for comparison with those of Schmidt and Bacskay (for up to $v'=5$ and $v''=5$) [56], using Eq. (5) and the wavenumber at which the forbidden $Q(0)$ transition would appear as the band wavenumber. It should be noted that slightly different $f_{v'v''}$ values would be obtained with a different choice of band wavenumber. Excellent agreement is shown for most bands, however some of the higher vibrational bands disagree by up to $\sim 50\%$ of the calculated values, as shown in Table 9.

5. Conclusion

Many perturbations are present in the $d^3\Pi_g$ state, and only those shown in Table 1 (involving the $d^3\Pi_g$, $v=4$ and $v=6$ levels) have been accounted for in these calculations. While many of the line positions in the new line list do not match experiment precisely, the intensities are an improvement on previously available data, where results have been based on the partly incorrect assignments made by Phillips and Davis [32]. The positions reported are also a slight improvement, mainly due to inclusion of the perturbation data of Bornhauser et al. [45,46]. A future investigation that could quantitatively account for all of the perturbations in the C_2 Swan system would be very beneficial. The calculated vibrational level lifetimes show good agreement with experimental and theoretical studies. The line list produced is an improvement over what is currently available, and will be of use to astronomers, materials scientists and combustion scientists in their analysis of the C_2 Swan system.

Acknowledgments

Support for this work was provided by a Research Project Grant from the Leverhulme Trust and a Department of Chemistry (University of York) studentship.

References

[1] Mayer P, O'Dell CR. Emission-band ratios in comet Rudnicki (1966e). Astrophys J 1968;153:951–62. http://dx.doi.org/10.1086/149721.
[2] Jackson W. The photochemical formation of cometary radicals. J Photochem 1976;5:107–18.
[3] Lambert DL, Danks AC. High-resolution spectra of C_2 Swan bands from comet West 1976 VI. Astrophys J 1983;268:428–46. http://dx.doi.org/10.1086/160969.
[4] Johnson JR, Fink U, Larson HP. 0.9−2.5 μm spectrum of comet West 1976 VI. Astrophys J 1983;270:769–77. http://dx.doi.org/10.1086/161168.
[5] Sorkhabi O, Blunt VM, Lin H, A'Hearn MF, Weaver HA, Arpigny C, et al. Using photochemistry to explain the formation and observation of C_2 in comets. Planet Space Sci 1997;45:721–30.
[6] Kaiser RI, Balucani N, Charkin DO, Mebel AM. A crossed beam and ab initio study of the C_2 ($X^1\Sigma_g^+/a^3\Pi_u$)+C_2H_2($X^1\Sigma_g^+$) reactions. Chem Phys Lett 2003;382:112–9. http://dx.doi.org/10.1016/j.cplett.2003.10.023.
[7] Souza SP, Lutz BL. Detection of C_2 in the interstellar spectrum of Cygnus OB2 number 12 (VI Cygni number 12). Astrophys J 1977;216:L49–51. http://dx.doi.org/10.1086/182507.
[8] Chaffee Jr. FH, Lutz BL. The detection of interstellar diatomic arbon toward Zeta Ophiuchi. Astrophys J 1978;221:L91–3, http://dx.doi.org/10.1086/182671.
[9] Green S. Interstellar chemistry: exotic molecules in space. Annu Rev Phys Chem 1981;32:103–38. http://dx.doi.org/10.1146/annurev.pc.32.100181.000535.
[10] Hobbs LM, Campbell B. Interstellar C_2 molecules toward Zeta Ophiuchi. Astrophys J 1982;254:108–10. http://dx.doi.org/10.1086/159711.
[11] Federman SR, Huntress Jr. WT. Diffuse interstellar clouds as a chemical laboratory - the chemistry of diatomic carbon species. Astrophys J 1989;338:140–6. http://dx.doi.org/10.1086/167187.
[12] Kaźmierczak M, Schmidt MR, Bondar A, Kreiowski J. Abundances and rotational temperatures of the C_2 interstellar molecule towards six reddened early-type stars. Mon Not R Astron Soc 2010;402:2548–58. http://dx.doi.org/10.1111/j.1365-2966.2009.16065.x.
[13] Casu S, Cecchi-Pestellini C. Excitation of C_2 in diffuse interstellar clouds. Astrophys J 2012;749:48. http://dx.doi.org/10.1088/0004-637X/749/1/48.
[14] Vardya MS. Atmospheres of very late-type stars. Annu Rev Astron Astrophys 1970;8:87–114. http://dx.doi.org/10.1146/annurev.aa.08.090170.000511.
[15] Querci F, Querci M, Kunde VG. Opacity probability distribution functions for electronic systems of CN, C_2 molecules including their stellar isotopic forms. Astron Astrophys 1971;15:256–74.
[16] Klochkova VG, Szczerba R, Panchuk VE. Optical spectrum of the infrared source IRAS 23304+6147. Astron Lett 2000;26:88–103. http://dx.doi.org/10.1134/1.20372.
[17] Hema BP, Pandey G, Lambert DL. The galactic R coronae borealis stars: the C_2 Swan bands, the carbon problem, and the $^{12}C/^{13}C$ ratio. Astrophys J 2012;747:102. http://dx.doi.org/10.1088/0004-637X/747/2/102.
[18] Grevesse N, Sauval AJ. A study of molecular lines in the solar photospheric spectrum. Astron Astrophys 1973;27:29–43.
[19] Brault JW, Testerman L, Grevesse N, Sauval AJ, Delbouille L, Roland G. Infrared bands of C_2 in the solar photospheric spectrum. Astron Astrophys 1982;108:201–5.
[20] Kaiser RI. Experimental investigation on the formation of carbon-bearing molecules in the interstellar medium via neutral–neutral reactions. Chem Rev 2002;102:1309–58.
[21] Gaydon A. The spectroscopy of flames. Wiley; 1957.
[22] Bleekrode R, Nieuwpoort WC. Absorption and emission measurements of C_2 and CH electronic bands in low-pressure oxyacetylene flames. J Chem Phys 1965;43:3680–7.
[23] Baronavski AP, McDonald JR. Measurement of C_2 concentrations in an oxygen-acetylene flame: an application of saturation spectroscopy. J Chem Phys 1977;66:3300–1.
[24] Goulay F, Nemes L, Schrader PE, Michelsen HA. Spontaneous emission from C_2($d^3\Pi_g$) and C_3($A^1\Pi_u$). Mol Phys 2010;108:1013–25. http://dx.doi.org/10.1080/00268971003627824.
[25] Nemes L, Irle S, Spectroscopy. dynamics and molecular theory of carbon plasmas and vapors: advances in the understanding of the most complex high-temperature elemental system. World Scientific; 2011.
[26] Herzberg G, Lagerqvist A, Malmberg C. New electronic transitions of the C_2 molecule in absorption in the vacuum ultraviolet region. Can J Phys 1969;47:2735–43. http://dx.doi.org/10.1139/p69-335.
[27] King RB. Relative transition probabilities of the Swan bands of carbon. Astrophys J 1948;108:429–33. http://dx.doi.org/10.1086/145078.
[28] Phillips JG. Laboratory determination of relative transition probabilities of diatomic molecules. II. The Swan system $^3\Pi_g$-$^3\Pi_u$ of the C_2 molecule. Astrophys J 1957;125:153–62. http://dx.doi.org/10.1086/146290.
[29] Hagan LG. The absolute intensity of C_2 Swan bands. Thesis. Berkeley: California University, Lawrence Radiation Lab.; 1963.
[30] Mentall JE, Nicholls RW. Absolute band strengths for the C_2 Swan system. Proc Phys Soc 1965;86:873–6. http://dx.doi.org/10.1088/0370-1328/86/4/326.
[31] Tyte DC, Innanen SH, Nicholls RW. Identification atlas of molecular spectra, vol. 5. The C_2 d $^3\Pi_g$-$a^3\Pi_u$ Swan system. Technical Report; York University, Toronto; 1967.
[32] Phillips JG, Davis SP. The Swan system of the C_2 molecule, The spectrum of the HgH molecule. University of California Press; 1968.
[33] Danylewych LL, Nicholls RW. Intensity measurements on the C_2 (d $^3\Pi_g$-$a^3\Pi_u$) Swan band system. I. Intercept and partial band methods. Proc R Soc Lond A Math Phys Sci 1974;339:197–212.
[34] Huber K, Herzberg G. Molecular spectra and molecular structure, Volume IV: constants of diatomic molecules. Van Nostrand Reinhold; 1979.
[35] Amiot C. Fourier spectroscopy of the $^{12}C_2$, $^{13}C_2$, and $^{12}C^{13}C$ (0-0) Swan bands. Astrophys J Suppl Ser 1983;52:329–40. http://dx.doi.org/10.1086/190870.
[36] Curtis MC, Sarre PJ. High-resolution laser spectroscopy of the Swan system ($d^3\Pi_g$-$a^3\Pi_u$) of C_2 in an organic halide-alkali metal flame. J Mol Spectrosc 1985;114:427–35. http://dx.doi.org/10.1016/0022-2852(85)90235-8.

[37] Suzuki T, Saito S, Hirota E. Doppler-limited dye laser excitation spectrum of the C_2 Swan band ($\nu'-\nu''=1-0$). J Mol Spectrosc 1985;113:399–409. http://dx.doi.org/10.1016/0022-2852(85);90278-4.

[38] Dhumwad RK, Patwardhan AB, Kulkarni VT, Savadatti MI. Investigations in (0-0) isotopic bands of the C_2 Swan system. J Mol Spectrosc 1981;85:177–88. http://dx.doi.org/10.1016/0022-2852(81)90317-9.

[39] Prasad CVV, Bernath PF. Fourier transform spectroscopy of the Swan ($d^3\Pi_g$-$a^3\Pi_u$) system of the jet-cooled C_2 molecule. Astrophys J 1994;426:812–21. http://dx.doi.org/10.1086/174118.

[40] Lloyd GM, Ewart P. High resolution spectroscopy and spectral simulation of C_2 using degenerate four-wave mixing. J Chem Phys 1999;110(1):385–92.

[41] Tanabashi A, Amano T. New identification of the visible bands of the C_2 Swan system. J Mol Spectrosc 2002;215:285–94.

[42] Tanabashi A, Hirao T, Amano T, Bernath PF. The Swan system of C_2: a global analysis of Fourier transform emission spectra. Astrophys J Suppl Ser 2007;169:472–84.

[43] Rousselot P, Jehin E, Manfroid J, Hutsemékers D. The $^{12}C_2/^{12}C^{13}C$ isotopic ratio in comets C/2001 Q4 (NEAT) and C/2002 T7 (LINEAR). Astron Astrophys 2012;545:A24. http://dx.doi.org/10.1051/0004-6361/201219265.

[44] Li G, Harrison JJ, Ram RS, Western CM, Bernath PF. Einstein A coefficients and absolute line intensities for the $E^2\Pi$-$X^2\Sigma^+$ transition of CaH. J Quant Spectrosc Radiat Transfer 2012;113:67–74.

[45] Bornhauser P, Knopp G, Gerber T, Radi P. Deperturbation study of the $d^3\Pi_g$, $v'=4$ state of C_2 by applying degenerate and two-color resonant four-wave mixing. J Mol Spectrosc 2010;262: 69–74. http://dx.doi.org/10.1016/j.jms.2010.05.008.

[46] Bornhauser P, Sych Y, Knopp G, Gerber T, Radi PP. Shedding light on a dark state: the energetically lowest quintet state of C_2. J Chem Phys 2011;134:044302. http://dx.doi.org/10.1063/1.3526747.

[47] Yeung SH, Chan MC, Wang N, Cheung AC. Observation of the $\Delta v=-4$ vibronic sequence of the C_2 Swan system. Chem Phys Lett 2013;557:31–6. http://dx.doi.org/10.1016/j.cplett.2012.11.092.

[48] Western CM, PGOPHER, a program for simulating rotational structure (v. 7.1.108); 2010 〈http://pgopher.chm.bris.ac.uk〉.

[49] Brown J, Merer A. Lambda-type doubling parameters for molecules in Π electronic states of triplet and higher multiplicity. J Mol Spectrosc 1979;74(3):488–94. http://dx.doi.org/10.1016/0022-2852(79)90172-3.

[50] Hirota E, Brown J, Hougen J, Shida T, Hirota N. Symbols for fine and hyperfine-structure parameters. Pure Appl Chem 1994;66(3): 571–6. http://dx.doi.org/10.1351/pac199466030571.

[51] Amiot C, Chauville J, Maillard JP. New analysis of the C_2 Ballik-Ramsay system from flame emission spectra. J Mol Spectrosc 1979;75(1):19–40.

[52] Bernath P. Spectra of atoms and molecules. 2nd ed.Oxford University Press; 2005.

[53] Larsson M. Conversion formulas between radiative lifetimes and other dynamical variables for spin-allowed electronic transitions in diatomic molecules. Astron Astrophys 1983;128:291–8.

[54] Le Roy RJ. Level 8.0: a computer program for solving the radial Schrödinger equation for bound and quasibound Levels. University of Waterloo Chemical Physics Research Report: University of Waterloo; 2007.

[55] Kokkin DL, Bacskay GB, Schmidt TW. Oscillator strengths and radiative lifetimes for C_2: Swan, Ballik-Ramsay, Phillips, and $d^3\Pi_g \leftarrow c^3\Sigma_u^+$ systems. J Chem Phys 2007;126:84302.

[56] Schmidt TW, Bacskay GB. Oscillator strengths of the Mulliken, Swan, Ballik-Ramsay, Phillips, and $d^3\Pi_g \leftarrow c^3\Sigma_u^+$ systems of C_2 calculated by MRCI methods utilizing a biorthogonal transformation of CASSCF orbitals. J Chem Phys 2007;127(23).

[57] Nakajima M, Joester JA, Page NI, Reilly NJ, Bacskay GB, Schmidt TW, et al. Quantum chemical study and experimental observation of a new band system of C_2, $e^3\Pi_g$-$c^3\Sigma_u^+$. J Chem Phys 2009;131: 044301.

[58] Werner HJ, Knowles PJ. An efficient internally contracted multiconfiguration–reference configuration interaction method. J Chem Phys 1988;89:5803–14.

[59] Knowles PJ, Werner HJ. An efficient method for the evaluation of coupling coefficients in configuration interaction calculations. Chem Phys Lett 1988;145:514–22.

[60] Werner HJ, Knowles PJ. A second order multiconfiguration SCF procedure with optimum convergence. J Chem Phys 1985;82: 5053–63.

[61] Knowles PJ, Werner HJ. An efficient second-order MC SCF method for long configuration expansions. Chem Phys Lett 1985;115(3): 259–67. http://dx.doi.org/10.1016/0009-2614(85)80025-7.

[62] Dunning Jr. TH. Gaussian basis sets for use in correlated molecular calculations. I. The atoms boron through neon and hydrogen. J Chem Phys 1989;90:1007–23.

[63] Kendall RA, Dunning Jr. TH, Harrison RJ. Electron affinities of the first-row atoms revisited. Systematic basis sets and wave functions. J Chem Phys 1992;96:6796–806.

[64] Woon DE, Dunning Jr. TH. Gaussian basis sets for use in correlated molecular calculations. V. Core-valence basis sets for boron through neon. J Chem Phys 1995;103:4572–85.

[65] Wilson AK, van Mourik T, Dunning Jr. TH. Gaussian basis sets for use in correlated molecular calculations. VI. Sextuple zeta correlation consistent basis sets for boron through neon. J Mol Struct: THEOCHEM 1996;388:339–49.

[66] de Jong WA, Harrison RJ, Dixon DA. Parallel Douglas–Kroll energy and gradients in NWChem: estimating scalar relativistic effects using Douglas–Kroll contracted basis sets. J Chem Phys 2001;114: 48–53.

[67] Douglas M, Kroll NM. Quantum electrodynamical corrections to the fine structure of helium. Ann Phys 1974;82:89–155.

[68] Hess BA. Applicability of the no-pair equation with free-particle projection operators to atomic and molecular structure calculations. Phys Rev A 1985;32:756–63. http://dx.doi.org/10.1103/PhysRevA.32.756.

[69] Hess BA. Relativistic electronic-structure calculations employing a two-component no-pair formalism with external-field projection operators. Phys Rev A 1986;33:3742–8. http://dx.doi.org/10.1103/PhysRevA.33.3742.

[70] Mitrushchenkov A, Werner HJ. Calculation of transition moments between internally contracted MRCI wave functions with non-orthogonal orbitals. Mol Phys 2007;105(9):1239–49. http://dx.doi.org/10.1080/00268970701326978.

[71] Werner HJ, Knowles PJ, Lindh R, Manby FR, Schütz M, Celani P, et al. MOLPRO, version 2006.1, a package of ab initio programs; 2006.

[72] Le Roy RJ. RKR1 2.0: a computer program implementing the first-order RKR method for determining diatomic molecule potential energy functions. University of Waterloo Chemical Physics Research Report: University of Waterloo; 2004.

[73] Rydberg R. Graphische darstellung einiger bandenspektroskopischer ergebnisse. Z Phys 1932;73:376–85. http://dx.doi.org/10.1007/BF01341146.

[74] Rydberg R. Uber einige potentialkurven des quecksilberhydrids. Z Phys 1933;80:514–24. http://dx.doi.org/10.1007/BF02057312.

[75] Klein O. Zur berechnung von potentialkurven für zweiatomige moleküle mit hilfe von spektraltermen. Z Phys 1932;76: 226–35. http://dx.doi.org/10.1007/BF01341814.

[76] Rees ALG. The calculation of potential-energy curves from band-spectroscopic data. Proc Phys Soc 1947;59:998–1008. http://dx.doi.org/10.1088/0959-5309/59/6/310.

[77] Callomon JH, Gilby AC. New observations on the Swan bands of C_2. Can J Phys 1963;41(7):995–1004. http://dx.doi.org/10.1139/p63-105.

[78] Douay M, Nietmann R, Bernath PF. The discovery of two new infrared electronic transitions of C_2: $B^1\Delta_g$-$A^1\Pi_u$ and $B'^3\Sigma_g^-$-$A^1\Pi_u$. J Mol Spectrosc 1988;131:261–71. http://dx.doi.org/10.1016/0022-2852(88)90237-8.

[79] Phillips JG. Perturbations in the Swan system of the C_2 molecule. J Mol Spectrosc 1968;28:233–42. http://dx.doi.org/10.1016/0022-2852(68)90008-8.

[80] Naulin C, Costes M, Dorthe G. C_2 Radicals in a supersonic molecular beam. Radiative lifetime of the $d^3\Pi_g$ state measured by laser-induced fluorescence. Chem Phys Lett 1988;143: 496–500. http://dx.doi.org/10.1016/0009-2614(88)87402-5.

[81] Bauer W, Becker KH, Bielefeld M, Meuser R. Lifetime measurements on electronically excited $C_2(A^1\Pi_u)$ and $C_2(d^3\Pi_g)$ by laser-induced fluorescence. Chem Phys Lett 1986;123:33–6.